ACS Synthetic Biology
Research Article
Cite This: ACS Synth. Biol. 2019, 8, 1847−1857
pubs.acs.org/synthbio

# Displaced by Deceivers: Prevention of Biosensor Cross-Talk Is Pivotal for Successful Biosensor-Based High-Throughput Screening Campaigns

Lion Konstantin Flachbart,[†] Sascha Sokolowsky,[†] and Jan Marienhagen*[,†,‡]

[†]Institute of Bio- and Geosciences, IBG-1: Biotechnology, Forschungszentrum Jülich, D-52425 Jülich, Germany
[‡]Institute of Biotechnology, RWTH Aachen University, Worringer Weg 3, D-52074 Aachen, Germany

Supporting Information

**ABSTRACT:** Transcriptional biosensors emerged as powerful tools for protein and strain engineering as they link inconspicuous production phenotypes to easily measurable output signals such as fluorescence. When combined with fluorescence-activated cell sorting, transcriptional biosensors enable high throughput screening of vast mutant libraries. Interestingly, even though many published manuscripts describe the construction and characterization of transcriptional biosensors, only very few studies report the successful application of transcriptional biosensors in such high-throughput screening campaigns. Here, we describe construction and characterization of the *trans*-cinnamic acid responsive transcriptional biosensor pSenCA for *Escherichia coli* and its application in a FACS based screen. In this context, we focus on essential methodological challenges during the development of such biosensor-guided high-throughput screens such as biosensor cross-talk between producing and nonproducing cells, which could be minimized by optimization of expression and cultivation conditions. The optimized conditions were applied in a five-step FACS campaign and proved suitable to isolate phenylalanine ammonia lyase variants with improved activity in *E. coli* and *in vitro*. Findings from this study will help researchers who want to profit from the unmatched throughput of fluorescence-activated cell sorting by using transcriptional biosensors for their enzyme and strain engineering campaigns.

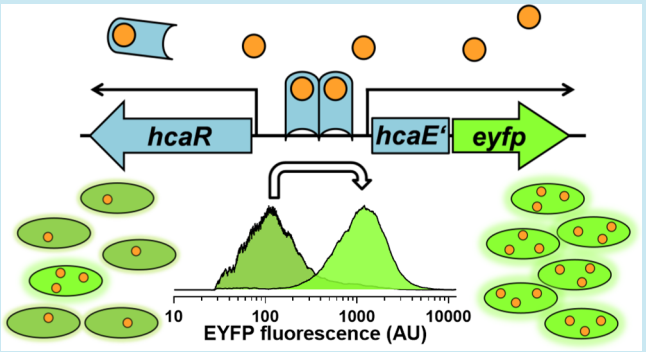


**KEYWORDS:** *transcriptional biosensor, library screening, product sensing, fluorescence-activated cell sorting, protein engineering, directed evolution*

Genetically encoded biosensors represent powerful tools in strain and protein engineering as they enable the high-throughput screening of large variant libraries by linking an often inconspicuous production phenotype to a readily detectable output signal.[1] In the past years, different biosensor concepts were introduced, namely, transcription factor (TF)-based biosensors, Förster resonance energy transfer (FRET) biosensors, as well as RNA-based biosensors.[2] Especially TF-based biosensors received a lot of attention as they are easy to construct and result in a relatively strong fluorescence signal.[3] Biosensors of this type take advantage of transcriptional regulator proteins, which specifically bind the molecule of interest and drive or repress expression of a reporter gene (usually encoding for a fluorescent protein or a selection marker). Examples for the application of these TF-based sensor-selector systems include screening campaigns for identifying improved producers from mutant libraries and selecting for suitable synthetic pathway variants.[4,5] Additionally, biosensors find application in synthetic sensor-actuator systems to enable the dynamic feedback regulation of heterologous pathways.[6−8] In combination with fluorescence activated cell sorting (FACS), such transcriptional biosensors unleash their true potential as they allow for ultrahigh throughput screening on single cell level and isolation of producing single cells from very large libraries.[9−13]

However, when considering the larger number of biosensors constructed over the past couple of years, studies combining transcriptional biosensors with FACS are rather scarce. For the most part, published biosensor screening applications are limited to agar plate or microtiter plate screenings, or the constructed and characterized biosensors are not put to any use at all. The transition from biosensor construction/characterization to meaningful applications involving FACS could be hampered by several factors. For instance, the engineered organism carrying the biosensor might provide a good fluorescence response in cultures, but give only a heterogeneous fluorescence response at the single cell level

**Received:** April 3, 2019
**Published:** July 3, 2019




DOI: 10.1021/acssynbio.9b00149
ACS Synth. Biol. 2019, 8, 1847−1857

prohibiting any FACS-based screening.[14] In addition, diffusion of the target metabolite from strong producing cells to weak or nonproducing strain variants could result in the isolation of mainly false-positive clones, demanding an individual and thus laborious and expensive characterization of many individual clones.

In this manuscript, we present suitable strategies by which these causes of failure can be efficiently tackled to yield robust and reliable biosensor-based FACS-ultrahigh-throughput screenings for protein and metabolic engineering campaigns. In this context, we describe construction and application of a transcriptional phenylpropanoid biosensor, which was used to engineer an ammonia lyase in *E. coli*.

## MATERIALS AND METHODS

**Bacterial Strains, Plasmids, Media, and Growth Conditions.** All bacterial strains and plasmids used in this study and their relevant characteristics are listed in Supplementary Table S1. For recombinant DNA work and library construction, *E. coli* DH5α and *E. coli* TOP10 (Thermo Fisher Scientific, Waltham, MA, USA) were used, respectively. For recovery after electroporation, SOC-medium (super optimal broth with catabolite repression) was used (20 g/L tryptone, 5 g/L yeast extract, 0.6 g/L NaCl, 0.2 g/L KCl, 10 mM MgCl/$MgSO_4$, and 20 mM glucose, pH 7). All strains were routinely cultivated at 37 °C on plates or in liquid culture in either Lysogeny broth (LB) medium (10 g/L tryptone, 10 g/L NaCl, and 5 g/L yeast extract) or Yeast nitrogen base (YNB) medium containing carbenicillin (50 μg/mL) or kanamycin (25 μg/mL), where appropriate.[15] For the preparation of 1 l of YNB medium, 100 mL of ten-times-concentrated YNB, containing 5.1% (cultivations 48 well and 96 well microtiter plates) or 12.6% (protein expressions) glycerol was added to 900 mL YNB base medium. YNB base medium contained 6 g/L $K_2HPO_4$, 3 g/L $KH_2PO_4$, and 10 g/L 3-(*N*-morpholino)propanesulfonic acid (MOPS), pH 7. As *E. coli* DH10B is leucine auxotroph, L-leucine was supplemented to a final concentration of 2 mM for all cultivations using YNB-medium.[16]

Online monitoring of growth and formation of fluorescence was performed in 48 well microtiter FlowerPlates (FPs) using the BioLector cultivation system (m2p-laboratories GmbH, Baesweiler, Germany).[17,18] Formation of biomass was recorded as the backscatter light intensity (wavelength 620 nm; signal gain factor 25). The enhanced yellow fluorescence protein (EYFP) fluorescence was measured as fluorescence emission at 532 nm (signal gain factor of 30) after excitation at a wavelength of 510 nm. Specific fluorescence was calculated as 532 nm fluorescence per 620 nm backscatter using Biolection software version 2.2.0.6 (m2p-laboratories GmbH, Baesweiler, Germany).

The *trans*-cinnamic acid (CA) and *p*-coumaric acid (pHCA) production assays were performed using single colonies from fresh plates or 10 μL from a fresh glycerol culture to inoculate LB medium in 96 well V-bottom plates (BRAND GMBH + CO KG, Wertheim, Germany) with a total volume of 200 μL per well. Precultures were cultivated for 18 h (single colonies) or 8 h (inoculation from glycerol culture) in a Multitron Pro HT Incubator (Infors AG, Bottmingen, Suisse, 37 °C, 900 rpm, 75% humidity, 3 mm throw). Of this preculture, 100 μL were used to inoculate 900 μL YNB medium followed by 20 h incubation in the same Incubator. Subsequently, YNB precultures were cooled to 25 °C and 100 μL preculture were used to inoculate 900 μL YNB medium containing 130 μM L-arabinose and either 3 mM L-phenylalanine or 3 mM L-tyrosine, respectively. After 16 h of cultivation (25 °C, 900 rpm, 75% humidity, 3 mm throw), product titers were determined.

**Molecular Biology.** *Standard Techniques for Molecular Cloning.* Polymerase chain reactions, DNA restrictions and ligations were performed according to standard protocols.[19] Enzymes were obtained from Thermo Fisher Scientific (Waltham, MA, USA) and used following the manufacturer's recommendations. Genes were amplified by PCR using Pfu UltraII polymerase (Agilent, Santa Clara, CA, USA). Cloning of the amplified PCR products was performed using restriction enzyme digestion and subsequent ligation or Gibson assembly.[20] Synthesis of oligonucleotides and sequencing of DNA using Sanger sequencing were performed by Eurofins MWG Operon (Ebersberg, Germany). All oligonucleotides used in this study are listed in Supplementary Table S2.

*Error-Prone PCR and Ammonia Lyase Library Construction.* The $xal_{Tc}$ gene was amplified from plasmid pCBJ296 using the Clontech Diversify kit (Takara Bio Europe, Saint-Germain-en-Laye, France) incorporating 2.3 or 4.6 mutations/kb and assembled with pBAD plasmid, previously amplified using PCR, using Gibson assembly. The resulting plasmid library was purified and transformed into One Shot TOP10 electrocompetent *E. coli* cells according to the manufacturer's recommendations. Plasmid preparations were performed using Midi kits according to the manufacturer's recommendation (Qiagen, Hilden, Germany). The plasmid library was retransformed into *E. coli DH10B* Δ*hcaREFCBD* pSenCA. Preparation of electrocompetent cells and electroporation of the plasmid library was performed as described elsewhere.[21]

*Chromosomal Deletions.* Deletion of chromosomal genes was performed using Lambda (λ)-Red recombineering.[22,23] Here, the recently published plasmid pSIJ8 was used according to the published protocol instead of the original two plasmid approach described by Datsenko and Wanner.[24,25]

**Fluorescence Activated Cell Sorting (FACS).** Single-cell fluorescence was determined and cell sortings were performed using a BD FACSAria II cell sorter (BD Biosciences, Franklin Lakes, NJ, USA) equipped with a 70 μm nozzle and run with a sheath pressure of 70 psi. A 488 nm blue solid laser was used for excitation. Forward-scatter characteristics (FSC) were recorded as small-angle scatter and side-scatter characteristics (SSC) were recorded as orthogonal scatter of the 488 nm laser. A 502 nm long-pass and 530/30 nm band-pass filter combination enabled EYFP fluorescence detection. Prior to data acquisition, debris and electronic noise were excluded from the analysis by electronic gating in the FSC-H against SSC-H plot. Another gating step was performed on the resulting population in the FSC-H against FSC-W plot to exclude doublets. Fluorescence acquisition was always performed with the population resulting from this two-step gating. For sorting applications, cells were diluted to an $OD_{600}$ below 0.1 where necessary using YNB base buffer, and 200 000 cells were sorted into 5 mL reaction tubes (Eppendorf AG, Hamburg, Germany), prefilled with 3 mL LB medium using an in-house built adapter for 5 mL reaction tubes that was described earlier.[26] To minimize residual sheath fluid in the recovery tube, sorted cells were centrifuged (10 min, 3000*g*, 4 °C), after removal of 3 mL supernatant and addition of 4.5 mL fresh LB medium, regeneration was performed (16 h, 37 °C, 170 rpm.) Sort precision was always set to purity setting and


DOI: 10.1021/acssynbio.9b00149
ACS Synth. Biol. 2019, 8, 1847−1857

the total event rate while sorting never exceeded 16 000 events per second. FACSDiva 7.0.1 (BD Biosciences, San Jose, USA) was used for FACS control and data analysis. FlowJo for Windows 10.4.2 (FlowJo, LLC, Ashland, OR, USA) and Prism 7.04 (GraphPad Software, San Diego, CA, USA) were used to produce high-resolution graphics of FACS data.

**Protein Purification and Enzyme Assays.** Selected $Xal_{Tc}$ encoding genes ($xal_{Tc}$) were recloned to enable their expression as fusion proteins with an N-terminal hexa histidine (His6)-tag in *E. coli* DH10B Δ*hcaREFCBD*. Single colonies were used to inoculate 5 mL LB and grown at 37 °C for 4 h. Afterward, 500 μL culture was used to inoculate 15 mL YNB (0.51% glycerol as carbon source) precultures. After 16 h of cultivation at 37 °C, these precultures were used to inoculate 100 mL YNB (1.2% glycerol as carbon source) cultures to an $OD_{600}$ of 0.2, which were cultivated (2 h, 37 °C, and 130 rpm) prior to the addition of L-arabinose to a final concentration of 1.3 mM. Gene expression was performed (20 h, 25 °C, and 130 rpm) and cells were harvested (15 min, 4000*g*, 4 °C). After resuspension in 15 mL sonication buffer (50 mM Tris-HCl, 500 mM NaCl, 10% glycerol, pH 7.5) cells were disrupted using an ultrasonic cell disruptor (Branson Ultrasonics Corporation, Danbury, CT, USA, eight sonication cycles of 30 s, 4 °C, duty cycle 34 and output control 8). From this, crude extracts were prepared by centrifugation in an Avanti J25 centrifuge (Beckmann Coulter Life Sciences, Indianapolis, IN, USA. 19 000 rcf, 45 min, 4 °C using a JA25.5 rotor). The supernatant was applied to a gravity flow column filled with Nickel-nitrilotriacetic acid (Ni-NTA) affinity agarose (Qiagen, Hilden, Germany, 1 mL bed volume). Protein loaded onto the column was washed subsequently with 10 mL sonication buffer and 10 mL wash buffer (sonication buffer with 30 mM imidazole) prior to elution with 3 mL elution buffer (sonication buffer with 300 mM imidazole) in 500 μL fractions. Protein containing fractions were pooled and the protein solution was transferred to a hydrated Slide-A-Lyzer dialysis cassette (Thermo Fisher Scientific, Schwerte, Germany, molecular cutoff of 10 kDa) and placed in 1 L dialysis buffer/assay buffer (50 mM Tris-HCl, pH 7.5 at 30 °C, with 150 mM NaCl and 10% glycerol). Dialysis was performed (20 h, 4 °C, 30 rpm) and enzyme assays were always performed directly after protein purification.

Enzyme assays were performed in 96 well plates with UV-transparent, flat bottom (Corning, New York, USA) in a Tecan M1000 plate reader (Tecan Group, Maennedorf, Switzerland), by following the increase in absorbance at 276 nm (CA) or 310 nm (pHCA). Twenty μg purified enzyme was transferred to each well and warmed to 30 °C for 60 s. Directly afterward, the substrate was added to a final volume of 200 μL using an E4XLS 100−1200 μL multichannel pipet (Rainin Mettler-Toledo, Giessen, Germany, three mixing steps, 100 μL mixing volume). Product formation was linear in the 80 s used to determine the initial product formation rate and proportional to the protein concentration used. No product formation was detected in absence of substrate or purified enzyme.

**Chemical Analyses.** All standards were purchased from Sigma-Aldrich (St. Louis, MO, USA). CA and pHCA concentrations in cell-free cultures were determined using high performance liquid chromatography (HPLC) 1260 Infinity system equipped with an Infinity Diode Array Detector module (Agilent, Santa Clara, CA, USA). For this, 250 μL culture broth were centrifuged in 96 well V-bottom plates (BRAND GMBH + CO KG, Wertheim, Germany) in a Heraeus Multifuge X3 centrifuge (Heraeus, Hanau, Germany, 30 min, 6000*g* and 8 °C) and 200 μL supernatant was transferred to a new 96 well V-bottom plate and directly applied to the HPLC (8 °C sample chamber temperature). LC separation of 2 μL samples was carried out with a Kinetex 1.7u C18 100-Å-pore-size column (Phenomenex, Torrance, CA, USA, 50 mm by 2.1 mm [internal diameter], 40 °C). For elution, 2% acetic acid (solvent A) and acetonitrile supplemented with 2% acetic acid (solvent B) were used as the mobile phases at a flow rate of 1 mL/min. A gradient was used, where the amount of solvent B was changed over the course of analysis (min 0 to 5, 15% to 90%; minute 5 to 5.5, 90% to 15%). CA and pHCA were detected by determining the absorbance at 295 and 310 nm, respectively, and concentrations were calculated using an appropriate standard curve.

**Bioinformatic Methods.** Dose−response data of the pSenCA biosensor construct was fit using the [Agonist] *vs* response function (variable slope) of Prism 7.04 (GraphPad Software, San Diego, CA, USA) with a constraint of the minimal fold induction ($\mu_{min}$) to 1.

$$\mu(I) = \mu_{min} + \frac{I^h \times (\mu_{max} - \mu_{min})}{(I^h + EC50^h)}$$

$\mu$, fold induction (also referred to as induction factor); $I$, inducer concentration; $h$, Hill coefficient/Hill slope; EC50, inducer concentration resulting in an induction of 50% $\mu_{max}$.

For the DNA sequence analysis of isolated $xal_{Tc}$ variants, all DNA sequences obtained from Eurofins MWG Operon were aligned with the original $xal_{Tc}$ sequence for identifying single nucleotide polymorphisms using the Clonemanager Professional software, version 9.51 (Scientific & Educational Software, Denver, CO, USA).

## RESULTS

**Construction and Characterization of the *trans*-Cinnamic Acid Biosensor pSenCA.** In bacteria, plants and fungi, ammonia lyases catalyze the nonoxidative deamination of the aromatic amino acids L-Phe (then best referred to as phenylalanine ammonia lyases, PALs; EC 4.3.1.24) and L-Tyr (then best referred to as tyrosine ammonia lyases, TALs; EC 4.3.1.23) yielding the phenylpropanoids *trans*-cinnamic acid (CA) or *p*-coumaric acid (pHCA), respectively.[27] This reaction represents the committed step in the biosynthesis of biotechnologically and pharmaceutically interesting polyphenols such as flavonoids, stilbenes, and lignans.[28,29] The biotechnological production of plant polyphenols using microorganisms requires the functional implementation of whole plant pathways into the producing cells.[30,31] In the context of engineering microorganisms for this purpose, generally low PAL- and TAL-activities were identified to be limiting the overall performance of the heterologous pathway in the respective microbial hosts.[32−35]

Driven by the motivation to engineer a PAL/TAL-enzyme toward increased activity for future applications in microbial plant polyphenol production, a biosensor for *trans*-cinnamic acid (CA) was designed and constructed. *E. coli* can catabolize a broad range of aromatic compounds including phenylpropionic acid (PP) and phenylpropanoids such as CA, *via* a dioxygenolytic pathway, which is partly encoded by the *hca* gene cluster.[36] Transcription of the *hca* cluster is induced by HcaR, which is a LysR type transcriptional regulator (LTTR),


DOI: 10.1021/acssynbio.9b00149
ACS Synth. Biol. 2019, 8, 1847−1857

in the presence of PP or CA.[37] Therefore, HcaR and its target promoter, $P_{hcaE}$ were selected for the construction of the plasmid-based CA biosensor pSenCA. The biosensor pSenCA harbors the regulator gene *hcaR*, under control of its native promoter, $P_{hcaR}$, the target promoter of HcaR, $P_{hcaE}$, and the first 45 bp of *hcaE* (*hcaE′*) transcriptionally fused to the *eyfp*-gene encoding for the enhanced yellow fluorescent protein (EYFP) (Figure 1A). This translational fusion was designed and constructed, because previous experiments with other regulator/promoter combinations showed that the interplay between the promoter and the 5′-end of the original open reading frame, which has been fine-tuned by evolution, enhance the overall biosensor response.[11] Earlier work on the *hca* operon showed strongly reduced expression of *hcaR* in cultivations with glucose as carbon and energy source, as the expression of *hcaR* is subject to catabolite repression.[38,39] Consequently, glycerol was used as sole carbon and energy source, resulting in a strong and homogeneous fluorescence response upon CA supplementation. To circumvent degradation of CA over the course of cultivation, the *hca* operon was subsequently deleted in *E. coli* DH10B, resulting in strain *E. coli* DH10B Δ*hcaREFCBD*. Cultures of *E. coli* DH10B Δ*hcaREFCBD* pSenCA (hereafter referred to as *E. coli* pSenCA), were supplemented with CA and also pHCA at different concentrations ranging from 1 μM to 1000 μM. The dose−response curve for CA was sigmoidal, with an operational range stretching from 3 μM CA to 300 μM CA thus spanning 2 orders of magnitude (Figure 1 B). The inducer concentrations resulting in 5% (EC5) and 95% (EC95) of the maximal fold induction are 7.5 μM CA and 126 μM CA, respectively. The maximal fold induction determined in specific EYFP fluorescence was 120-fold. In contrast, presence of pHCA in the culture medium triggered a minor fluorescence response (2-fold) of pSenCA, showing that this biosensor is indeed CA-specific.

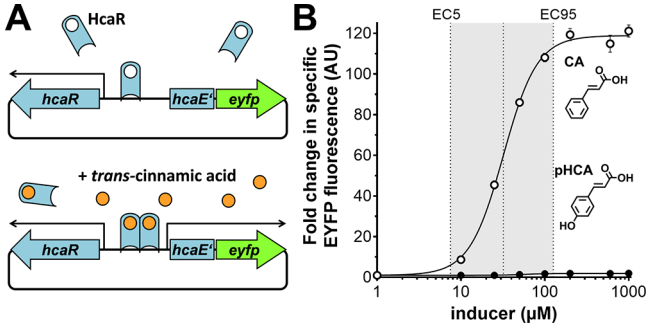


**Figure 1.** *trans*-Cinnamic acid biosensor pSenCA. (A) Schematic of the sensor principle. Upon binding of supplemented CA, the HcaR regulator undergoes conformational changes that enable binding to the target promoter $P_{hcaE}$ and activation of *hcaE′* and *eyfp* expression. (B) Dose−response plot, CA (circles) or pHCA (filled circles) were supplemented extracellularly in eight different concentrations ranging from 1 to 1000 μM. The biosensor response after 24 h is shown as fold change in specific EYFP fluorescence in comparison to the background fluorescence (no inducer). Error bars represent standard deviations calculated from three biological replicates. CA, *trans*-cinnamic acid; pHCA, *p*-coumaric acid; EC5, inducer concentration that results in 5% of maximal fold induction; EC95, inducer concentration resulting in 95% of maximal fold induction.

**Optimization of Heterologous Gene Expression Enables CA Production and Biosensor-Mediated Product Detection in *E. coli*.** Subsequently, a codon-optimized synthetic gene for the aromatic amino acid ammonia lyase $Xal_{Tc}$, originating from *Trichosporon cutaneum*, was introduced into *E. coli* pSenCA. In a previous study, this enzyme stood out

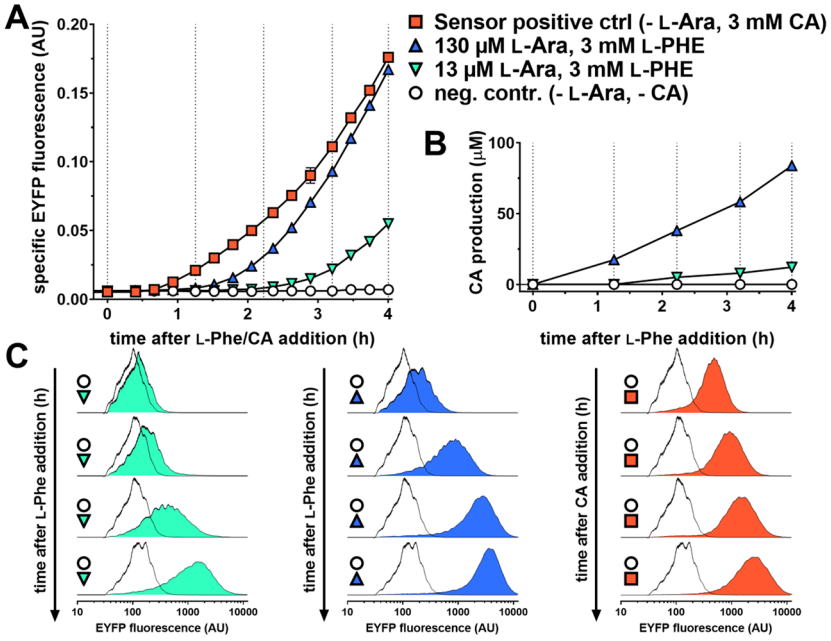


**Figure 2.** Influence of induction of heterologous $xal_{Tc}$ expression with 13 μM L-Ara or 130 μM L-Ara on biosensor response and CA production in *E. coli* pSenCA pBAD-$xal_{Tc}$. After cultivation for 3 h in the presence of different L-Ara concentrations, either 3 mM L-Phe (circles and triangles) or 3 mM CA (squares) was added. Samples were taken at four time points depicted by dotted lines (A) Specific fluorescence is shown (EYFP fluorescence × biomass formation$^{-1}$, arbitrary units). (B) CA concentration in *E. coli* culture supernatants. (C) FACS measurement of EYFP fluorescence of 62 000 representative single cells in the histogram representation. Abbreviations: CA, *trans*-cinnamic acid; L-Ara, L-arabinose; and L-Phe, L-phenylalanine.



DOI: 10.1021/acssynbio.9b00149
*ACS Synth. Biol.* 2019, 8, 1847−1857

among 21 other ammonia lyases as highly active enzyme having both PAL- and TAL-activities.[40] Here, the L-arabinose (L-Ara) inducible pBAD expression system was used for $xal_{Tc}$ expression in *E. coli* as it allows for tightly controlled and titratable heterologous gene expression.[41] For optimization of $xal_{Tc}$ expression in the resulting strain *E. coli* pSenCA pBAD-$xal_{Tc}$ at microtiter plate scale, five L-Ara concentrations (13 $\mu$M, 130 $\mu$M, 1.3 mM, 13 mM, and 130 mM) were evaluated. All cultivations were performed with supplementation of 3 mM L-Phe, which served as $Xal_{Tc}$ substrate. The performed microtiter plate cultivations in a biolector allowed for the monitoring of EYFP fluorescence over the whole cultivation time of 48 h (Supplementary Figure S1). Interestingly, low inducer concentrations (13 $\mu$M and 130 $\mu$M) ultimately resulted in the highest specific biosensor response, whereas induction of gene expression at higher L-Ara concentrations (1.3, 13, and 130 mM) appeared to impede formation of fluorescence. In addition, with increasing L-Ara concentrations, growth rate and final biomass formation were reduced. Since different L-Ara concentrations are not known to be problematic for the cellular metabolism, it was concluded that the reduced fluorescence formation is a consequence of the metabolic burden of high level $xal_{Tc}$ expression.[42] Therefore, cultivations with supplementation of 13 $\mu$M and 130 $\mu$M L-Ara were characterized in detail with regard to CA formation and pSenCA response to identify suitable conditions for FACS-based screenings. Noteworthy, heterologous $xal_{Tc}$-expression using 130 $\mu$M L-Ara yielded a fluorescence response close to the saturation of the biosensor, which was similar to the performed control experiments without $xal_{Tc}$-expression but supplementation of 3 mM CA (Figure 2A). Under these conditions, *E. coli* pSenCA pBAD-$xal_{Tc}$ accumulated 84 $\mu$M CA in the supernatant within 4 h of cultivation (Figure 2B). This means that induction of gene expression with 130 $\mu$M L-Ara would be too high for distinguishing improved $Xal_{Tc}$ variants from wild-type $Xal_{Tc}$ during FACS-based screening campaigns using pSenCA, but allows reliable discrimination of CA-producing cells from nonproducers. In contrast, induction of gene expression with 13 $\mu$M L-Ara leads to less pronounced fluorescence response far from biosensor saturation, enabling the isolation of more active $Xal_{Tc}$ variants from genetically diverse enzyme libraries (Figure 2A). Hence, consecutive rounds of FACS screening, first under "strong" gene expression conditions (130 $\mu$M L-Ara) to reliably enrich CA-producers, and then under "weak" gene expression conditions (13 $\mu$M L-Ara) to enable selection of the best variants within that pool of CA-producing cells could be a feasible FACS screening strategy.

**Prevention of Biosensor Cross-Talk Is a Prerequisite for Any FACS Applications Using pSenCA.** Many small molecules of biotechnological interest readily diffuse over biological membranes or are taken up by carrier-mediated transport (facilitated diffusion or active transport).[43] This aspect poses a major challenge during biosensor-based FACS-screenings as biosensor cross-talk between producing and nonproducing variants would lead to a high number of isolated false-positive variants. Induction of $xal_{Tc}$-expression in *E. coli* pSenCA pBAD-$xal_{Tc}$ with 13 $\mu$M L-Ara allows for a product titer of 12 $\mu$M CA after 4 h of cultivation after L-Phe addition, which might already promote an undesired pSenCA cross-talk. With the aim of detecting any pSenCA cross-talk and developing a cultivation strategy for minimizing this effect prior to conducting any FACS screenings, defined mixtures of *E. coli* pSenCA pBAD-$xal_{Tc}$ cells ($CA^+$) and *E. coli* pSenCA cells ($CA^-$) were analyzed by FACS over the course of cultivation time. In this experiment, a 50% $CA^+$/50% $CA^-$ mixed culture was inoculated to a starting $OD_{600}$ ($iOD_{600}$) of 0.5 and cultivated for 8 h (3 h $xal_{Tc}$ expression and 5 h cultivation after L-Phe addition) before the top 5% fluorescing cells were isolated by FACS. Performed colony-PCRs revealed that 30% of these cells did not carry pBAD-$xal_{Tc}$ (Supplementary Figure S2A). Reason for this could be either spontaneous mutations in pSenCA leading to constitutive *eyfp* expression in the $CA^-$ cells, or CA uptake from the supernatant by the $CA^-$ cells, which activated the biosensor. However, since none of the isolated $CA^-$ cells showed fluorescence in the absence of CA, it was concluded that the uptake of CA from the supernatant was the reason for the isolation of false positive $CA^-$ cells. These results indeed showed that pSenCA cross-talk between individual cells occurs, impeding any future FACS-screening campaigns.

Driven by the idea that reduction of the inoculum ($iOD_{600}$) might be useful strategy for minimizing biosensor cross-talk, four different $CA^+/CA^-$ ratios (20% $CA^+$/80% $CA^-$; 50% $CA^+$/50% $CA^-$; 80% $CA^+$/20% $CA^-$; 100% $CA^+$/0% $CA^-$) at four different $iOD_{600}$ (0.5; 0.1; 0.02; 0.004) were compared with regard to fluorescence at single cell level and FACS sorting efficiency (Figure 3). Noteworthy, the median fluorescence intensity of the culture with 100% $CA^+$ cells decreased with decreasing inoculum size, and a smaller population of highly fluorescing cells became apparent. This observation hints toward population heterogeneity with regard to either $xal_{Tc}$-expression or stochastic HcaR-binding events in the low-CA accumulation range and subsequent CA

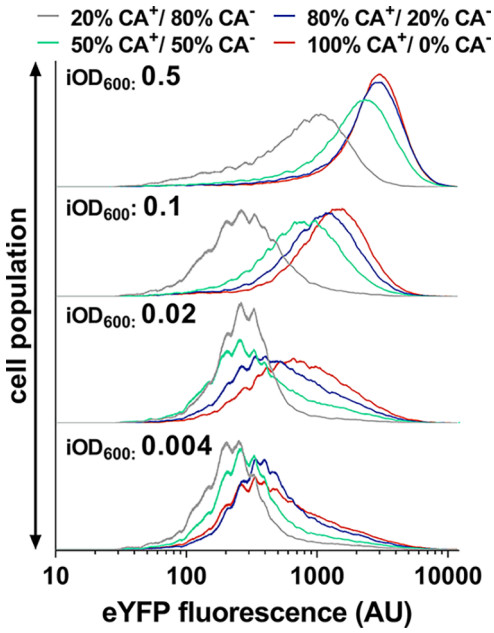


**Figure 3.** EYFP fluorescence of various mixed cultures of *trans*-cinnamic acid producing and nonproducing *E. coli* strains during cytometric analysis. All cultures were started using different inoculums ($iOD_{600}$) as indicated. All cultivations were performed in the in the presence of 13 $\mu$M L-arabinose for induction of heterologous $xal_{Tc}$ expression and 3 mM L-Phe as XAL-substrate always added 3 h after starting each cultivation. FACS measurements were performed 5 h after substrate addition. Strains: $CA^+$, *E. coli* pSenCA pBAD-$xal_{Tc}$; $CA^-$, *E. coli* pSenCA pBAD.



DOI: 10.1021/acssynbio.9b00149
*ACS Synth. Biol.* 2019, 8, 1847−1857

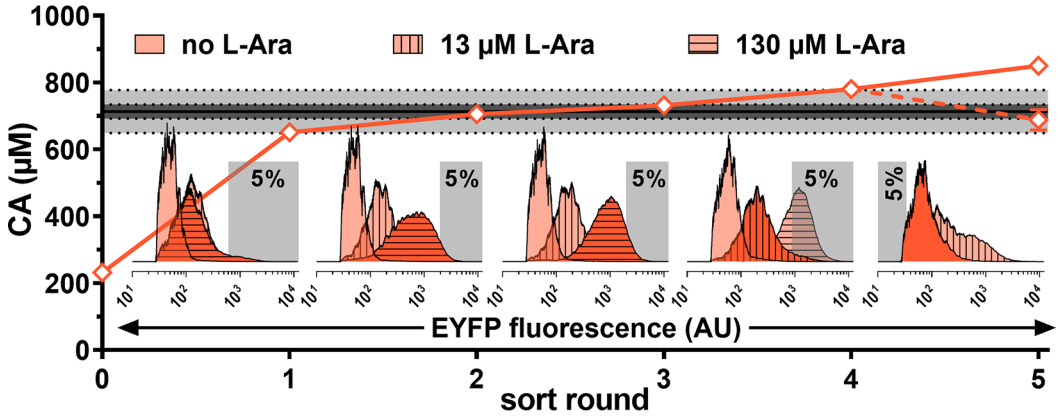


**Figure 4.** Stepwise enrichment of improved CA producers from a $xal_{Tc}$ library using biosensor-based FACS-screening. The continuous orange graph depicts the development of the CA titer of the $xal_{Tc}$ library at the culture level relative to the starting variant *E. coli* pSenCA pBAD-$xal_{Tc}$ (black line). The dashed orange graph depicts the CA titer development in a control experiment, in which another positive sorting (fluorescence) instead of the negative sorting (no fluorescence) was performed. The dark gray shading depicts the CA-titer range of one standard deviation from the $Xal_{Tc}$ starting variant, whereas light gray shading depicts the CA-titer range of three standard deviations. Histograms show the fluorescence distribution of the cultures of each cultivation step without induction of heterologous gene expression (no L-Ara) or substrate addition (no L-Phe) (histogram without pattern), with supplementation of 13 $\mu$M L-Ara and 3 mM L-Phe (vertical lines) and 130 $\mu$M L-Ara and 3 mM L-Phe added (horizontal lines). Conditions of each step leading to the eventually isolated $xal_{Tc}$ variants are highlighted in bright orange relative to the conditions only used as controls that are shown in dim orange. Gray boxes visualize the respective sorting gate set in each step: Step 1−4, positive sorts (isolation of the top 5% fluorescing events); Step 5, negative sort (isolation of the lower 5% fluorescing events). Cultivations for CA titer determination were always performed in triplicates, error bars depict the respective standard deviations. The dotted line depicts development of CA production for an additional round of positive sorting in step five (Supplementation of 13 $\mu$M L-Ara), which was performed in parallel for comparison. Abbreviations: CA, *trans*-cinnamic acid; L-Ara, L-arabinose; L-Phe, L-phenylalanine.

production in these otherwise genetically homogeneous cultures. In combination with the biosensor cross-talk, the observed heterogeneity provides an explanation for the homogeneous looking population at an $iOD_{600}$ of 0.5 as the increasing number of CA-producers among the 100% $CA^+$ cells also produced more CA, which was then taken up by the nonproducing cells. Consequently, with a decreasing share of $CA^+$ cells at different $CA^+/CA^-$ ratios and decreasing $iOD_{600}$ tested, the number of CA-producing cells was more and more reduced, resulting in a decreased median fluorescence of the respective cultures, but also a more pronounced small population of highly fluorescent CA-producing cells (Figure 3). This indicates that a reduced inoculum reduces the biosensor cross-talk between $CA^+$ and $CA^-$ cells presumably enabling for the efficient biosensor-guided isolation of $CA^+$ cells by FACS. Subsequently performed FACS experiments in which only the top 5% fluorescent cells of the 20% $CA^+$/80% $CA^-$ and 50% $CA^+$/50% $CA^-$ cultures with an $iOD_{600}$ of 0.02 or 0.004 were isolated and characterized, confirmed this assumption as all isolated cells were $CA^+$ cells (Supplementary Figure S2B−E).

**Directed Evolution of an Ammonia Lyase by Multistep FACS Screening.** The previously established and optimized gene expression and cultivation conditions were subsequently used to screen a diverse $XAL_{Tc}$ library for isolating enzyme variants with an improved activity in *E. coli*. For this purpose, a randomly mutated $xal_{Tc}$ library of $2.3 \times 10^6$ variants was constructed by subcloning of $xal_{Tc}$ error-prone PCR products into the pBAD vector, and transformation into electrocompetent *E. coli* pSenCA cells.

A multistep FACS enrichment strategy was performed in which always the top 5% fluorescent cells were collected and recultivated for the next enrichment step (Figure 4). During this campaign, the average CA production of the recovered cells in the culture was determined by HPLC after every step to judge successful enrichment of CA producing cells. The first FACS enrichment steps were performed under strong $xal_{Tc}$-induction conditions with supplementation of 130 $\mu$M L-Ara to reliably enrich CA producing variants. In parallel, during each round of enrichment, the respective *E. coli* cultures were also analyzed by FACS under weak $xal_{Tc}$-induction conditions (13 $\mu$M L-Ara) for comparison and also without any induction of $xal_{Tc}$ expression (no L-Ara) or addition of the $Xal_{Tc}$ substrate L-Phe for identifying false positive variants bearing spontaneous mutations leading to constitutive *eyfp* expression. In the course of the enrichments under strong $xal_{Tc}$-induction conditions, the CA titer increased from 232 to 651 $\mu$M (1st FACS-enrichment step), from 651 to 706 $\mu$M (2nd FACS-enrichment step), and from 706 to 734 $\mu$M (3rd FACS-enrichment step), respectively, without a detectable increase in fluorescence in the false positive controls (Figure 4). A subsequent fourth enrichment step was performed with lower induction of heterologous gene expression (13 $\mu$M L-Ara) for identifying the best CA producers in the enrichments. The strategy was changed as the third step with high induction of gene expression resulted only in a small increase of the CA titer by 28 $\mu$M. Presumably this was the case because most remaining cells in the third enrichment were already CA producers, promoting strong fluorescence under high induction of heterologous gene expression (130 $\mu$M L-Ara). Surprisingly, this fourth enrichment step in the presence of 13 $\mu$M L-Ara resulted in the occurrence of a pronounced fluorescent population as a shoulder in the histogram of the control FACS experiment without L-Ara or L-Phe, indicating that false positive variants were enriched under these conditions. Hence, an additional control experiment was performed, in which a fifth positive FACS screening of the library in the presence of 13 $\mu$M L-Ara (positive sort under weak induction conditions) was conducted (Figure 4, dotted line). As expected, a decreasing average CA-titer (688 $\mu$M CA)


DOI: 10.1021/acssynbio.9b00149
*ACS Synth. Biol.* 2019, 8, 1847−1857

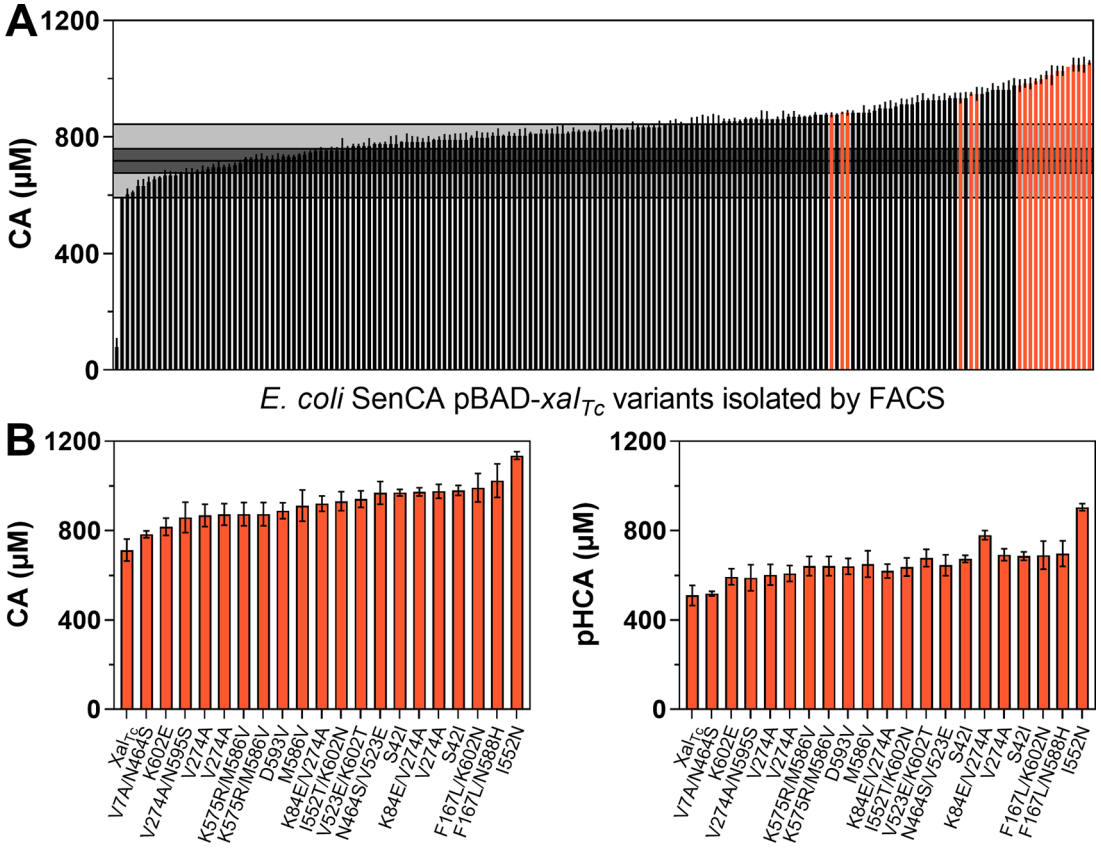


**Figure 5.** (A) *trans*-Cinnamic acid production of 183 FACS-isolated Xal$_{Tc}$ variants. Presented data are means of three cultivations and error bars depict standard deviations. The dark gray shading depicts the CA-titer range of one standard deviation from the Xal$_{Tc}$ starting variant, whereas light gray shading depicts the CA-titer range of three standard deviations. (WT cultivated as biological triplicates). Variants selected for a more detailed analysis are highlighted in orange. (B), CA (left) and pHCA (right) production of 19 strains selected during the initial characterization (Figure 5A), after retransformation of the respective pBAD*xal*$_{TcEc}$ plasmid. All cultivations were performed in biological triplicates, error bars depict the standard deviation. Abbreviations: CA, *trans*-cinnamic acid; pHCA, *p*-coumaric acid.

of the enriched culture was determined as the false positives variants were further enriched. The solution was a final negative FACS-step (no L-Ara and L-Phe supplementation) and sorting of the 5% least fluorescing cells to exclude false positive variants. This increased the average CA-titer of the library to 850 $\mu$M upon recultivation.

During the FACS campaign, the stepwise enrichment resulted in a culture of *E. coli* variants, which accumulated up to 20% more CA in the supernatant in comparison to a culture of the starting variant *E. coli* pSenCA pBAD-*xal*$_{Tc}$ that accumulates 713 $\mu$M CA. For comparison, prior to any FACS enrichment, the randomly mutated and unsorted Xal$_{Tc}$-library accumulated 232 $\mu$M CA, which is 70% less CA compared to the starting variant.

The *E. coli* cells recovered after the fifth enrichment step were spread on LB agar plates and 182 single colonies were individually cultivated and characterized with regard to their respective CA production capabilities (Figure 5A). These experiments revealed that 8% of these variants accumulated less CA compared to the starting variant, whereas 16% could not be distinguished from this control. In contrast, 76% of the strains accumulated significantly (>10%) more CA, with the upper 20% accumulating 30% to 50% more CA compared to the starting variant *E. coli* pSenCA pBAD-*xal*$_{Tc}$.

Subsequently, the pBAD-*xal*$_{Tc}$ plasmids of the 15 best variants and five randomly selected variants with significantly higher CA accumulation compared to the starting variant were isolated and retransformed into *E. coli* pSenCA to exclude the potential influence of undesired random genomic mutations (Figure 5A). The resulting strains were compared to *E. coli* pSenCA pBAD-*xal*$_{Tc}$ regarding their CA and pHCA accumulation from supplemented L-Phe and L-Tyr, respectively (Figure 5 B). In parallel, the DNA sequence of all 20 *xal*$_{Tc}$ variants was determined. All variants accumulated 10% to 60% more CA or pHCA in the supernatant when L-Phe or L-Tyr were supplemented, respectively. Interestingly, DNA sequencing revealed that 6 strains have mutations in the P$_{araB}$-promoter upstream of *xal*$_{Tc}$, whereas 14 variants exclusively carry mutations in the *xal*$_{Tc}$ open reading frame (Supplementary table S3).

Nonetheless, the increased CA titer of these 14 strains could be also due to improved heterologous expression of *xal*$_{Tc}$ and thus higher Xal$_{Tc}$ abundance and does not necessarily have to relate to altered enzyme kinetics of the enzyme. With the aim, to preclude any undesired expression effects, an *in vitro* characterization of seven Xal$_{Tc}$ variants with purified proteins was performed. Seven muteins, including Xal$_{Tc}$-F167L-K602N, Xal$_{Tc}$-N464S/V523E, Xal$_{Tc}$-F167L/N588H, Xal$_{Tc}$-I552N, Xal$_{Tc}$-V523E/K602T, Xal$_{Tc}$-I552T/K602N, and Xal$_{Tc}$-V274A were selected to determine enzyme kinetics *in vitro*. These variants accumulated the highest CA concentrations in the *in vivo* experiments and did not carry mutations in the *araC* gene or in the P$_{araBAD}$ promoter (except for Xal$_{Tc}$-I552N comprising P$_{araBAD}$-a10g). For the *in vitro* enzyme assays, all genes were


DOI: 10.1021/acssynbio.9b00149
ACS Synth. Biol. 2019, 8, 1847−1857

Table 1. Kinetic Characterization of Selected $Xal_{Tc}$ Muteins Obtained during the Biosensor-Based FACS Screening Campaign

| | PAL reaction | | TAL reaction | |
|---|---|---|---|---|
| $Xal_{Tc}$ variant | $K_m$ (mM) | $V_{max}$ ($\mu$mol min$^{-1}$ mg$^{-1}$) | $K_m$ (mM) | $V_{max}$ ($\mu$mol min$^{-1}$ mg$^{-1}$) |
| $Xal_{Tc}$ "wild type" | 6.1 ± 0.6 | 1.24 ± 0.04 | 0.9 ± 0.09 | 0.49 ± 0.02 |
| $Xal_{Tc}$-V274A | 6.6 ± 0.5 | 1.38 ± 0.04 | 0.7 ± 0.05 | 0.5 ± 0.01 |
| $Xal_{Tc}$-I552N | 5.3 ± 0.2 | 1.28 ± 0.02 | 0.7 ± 0.06 | 0.26 ± 0.01 |
| $Xal_{Tc}$-I552T/K602N | 5.3 ± 0.3 | 1.27 ± 0.03 | 0.9 ± 0.09 | 0.5 ± 0.02 |
| $Xal_{Tc}$-N464S/V523E | 5.1 ± 0.4 | 1.1 ± 0.03 | 0.7 ± 0.05 | 0.25 ± 0.01 |
| $Xal_{Tc}$-V523E/K602T | 5.0 ± 0.4 | 1.22 ± 0.03 | 0.6 ± 0.04 | 0.26 ± 0.01 |
| $Xal_{Tc}$-F167L/K602N | 4.9 ± 0.5 | 1.41 ± 0.04 | 0.7 ± 0.05 | 0.49 ± 0.01 |
| $Xal_{Tc}$-F167L/N588H | 4.8 ± 0.4 | 1.34 ± 0.04 | 0.6 ± 0.05 | 0.3 ± 0.01 |

individually recloned into the pBAD-N6XHIS vector allowing for the generation of N-terminally His-tagged fusions proteins and subsequent Ni-NTA affinity chromatography. Protein purification yielded 4−5 mg of pure protein as judged by SDS-PAGE analysis for enzyme assays (Supplementary Figure S3). Six of the seven muteins characterized in this detail exhibit an up to 12% increased $V_{max}$ and an increased affinity to the substrates L-Phe and L-Tyr, respectively, which explains the observed increased CA- and pHCA-titers (Table 1). Interestingly, mutein $Xal_{Tc}$-V274A does have a reduced affinity toward L-Phe (6.6 mM) but exhibits one of the highest $V_{max}$ of the mutein set (1.38 $\mu$mol min$^{-1}$ mg$^{-1}$). In contrast, $Xal_{Tc}$-F167L/K602N and $Xal_{Tc}$-F167L/N588H show the lowest $K_m$ for both L-Phe and L-Tyr (4.8 mM/4.9 mM and 0.7 mM/0.6 mM, respectively), while the $V_{max}$ is only increased for the deamination of L-Phe in comparison to the wild-type enzyme.

## DISCUSSION

Enzyme as well as strain engineering can be substantially accelerated when biosensor-based FACS screenings can be implemented as this technology enables screening of vast and genetically diverse libraries with a throughput that is orders of magnitude higher compared to other well-established screening strategies.[44] However, prerequisite for the application of this powerful screening technique is the availability of a suitable biosensor for the compound of interest, and detailed knowledge of the biosensor characteristics with regard to dynamic range, kinetics of the output signal, and operational range.

Characterization of the pSenCA biosensor designed and constructed in this study revealed a strong biosensor induction by CA in the micromolar range. In comparison to other TF based biosensors, the operational range of pSenCA is rather low. For example, the pJC1-lrp-brnF′-eyfp biosensor for *C. glutamicum* for L-methionine and the branched chain amino acids L-valine, L-leucine, and L-isoleucine is characterized by a maximal fold induction of 78 and an operational range from 0.2 mM to 23.5 mM (for L-methionine).[45] The lower operational range of pSenCA in comparison to pJC1-lrp-brnF′-eyfp can be explained by the role of the respective transcriptional regulators, HcaR and Lrp, in the microbial metabolism. Lrp activates the expression of the *brnFE* operon, encoding for the branched-chain amino acid exporter BrnFE, which is responsible for secretion of excess amino acids to avoid cytotoxic effects of elevated intracellular amino acid concentrations.[46] HcaR, in contrast, activates the expression of the *hca* gene cluster involved in the catabolism of aromatic acids, which can serve as valuable carbon and energy sources in absence of other more preferred substrates.[37,39] A strong expression at low inducer concentrations is therefore beneficial to compete with other microorganisms for such valuable resources.

However, despite a low operational range, a biosensor can be used in FACS screenings if screening conditions are selected, in which the expected product concentrations match with the biosensor characteristics. In the case of the directed $Xal_{Tc}$ evolution performed in this study, only the two lowest inducer concentrations for heterologous *xalTc*-expression enabled pSenCA-guided FACS screening. As alternative for optimizing cultivation conditions, the biosensor itself can be adapted. For example, alteration of the operational range of a transcriptional biosensor can be achieved by engineering the transcriptional regulator toward reduced affinity to the ligand, thereby enabling a graded fluorescence output for higher ligand concentrations.[47] This approach was followed recently to optimize the operational range of a whole-cell biosensor for the detection and quantification of the macrodiolide antibiotic pamamycin produced by *Streptomyces alboniger*.[48] By rational engineering of the binding pocket of the PamR2 repressor, a mutein with reduced affinity for pamamycin could be constructed, extending the upper detection limit of the sensor system from 1 mg/L to more than 5 mg/L.

Additionally, given that the constructed biosensor does not provide sufficient dynamic range, often because of incompatibility between the host strain and heterologous regulatory elements, the target promoter of the regulator incorporated in the sensor or the promoter of the regulator gene can be mutated. For example, a 3,4-dihydroxy benzoate responsive biosensor based on the *pcaU* gene under control of its promoter $P_{pcaU}$ from *Acinetobacter sp ADP1* was applied in *E. coli*.[49] By random mutagenesis, a library of 33 000 promoter mutants was constructed and subsequently screened using FACS. Applying positive and negative screening, three variants with improved dynamic range were isolated. Another example is the a biosensor comprised of PadR, a repressor specific for *p*-coumaric acid from *Bacillus subtilis*, and its cognate promoter in *E. coli*.[50] A sensor variant with improved dynamic range was constructed by screening a set of $P_{padR}$RBS mutants for variants with reduced expression of *padR*. In other cases where neither optimization of cultivation conditions nor adaptation of the biosensor is an option, identification of the most suitable time-point for the FACS screening during cultivation presents a possible solution to prevent saturation of the sensor system.

Cross-talk between producers and nonproducing cells as it could be observed in this study impedes any biosensor-based FACS screening if the metabolite in question can diffuse of biological membranes or is readily taken up by the microorganism. Dilution to a starting $OD_{600}$ of 0.004 and short cultivation times (<8 h) successfully suppressed cross-talk in our case, even with an excess of producing cells in the culture.



DOI: 10.1021/acssynbio.9b00149
ACS Synth. Biol. 2019, 8, 1847−1857

A possible alternative to dilution for preventing cross-talk is compartmentalization of individual strain variants in solution, *e.g.*, by emulsion droplets, which can be sorted in microfluidic devices. By coencapsulation of an *E. coli* strain carrying a *p*-coumaric acid-responsive biosensor and *p*-coumaric acid producing *Saccharomyces cerevisiae*, yeast cells with elevated *p*-coumaric acid production capabilities could be isolated from mixtures of different producer strains.[50] However, design and construction of droplet-based screening assays is most likely more laborious, and the sorting speed in microfluidic devices is usually limited to less than 500 cells per second when reasonable sort efficiencies are desired.[50,51] Recently, successful sorting of double emulsion droplets in a FACS device could be demonstrated, increasing the throughput of droplet sorting to 1000 cells per second.[52] When performing dilution assays in this study, a pronounced heterogeneity with respect to the fluorescent response could be detected, which was presumably caused by heterogeneous expression of the $xal_{Tc}$ gene. This heterogeneous expression in the presence of subsaturating L-Ara concentrations was described earlier and could be eliminated by expression of the L-Ara importer gene *araE* under control of either a constitutive *Lactococcus lactis* or an Isopropyl-$\beta$-D-thiogalactopyranosid-inducible *lac* promoter.[53,54]

## CONCLUSIONS

In this study, a transcriptional biosensor for the phenylpropanoid *trans*-cinnamic acid could be successfully designed, constructed, and applied in a high-throughput FACS screening campaign. Key to success was a detailed characterization of the biosensor in combination with fine-tuning of cultivation and screening conditions to overcome hurdles such as biosensor cross-talk, which impede the successful application of more biosensors in the field of protein engineering or strain development. We believe that the strategies outlined in this article will help others to also develop elegant biosensor-based screening campaigns using the high-throughput capabilities of FACS.

## ASSOCIATED CONTENT

### Supporting Information

The Supporting Information is available free of charge on the ACS Publications website at DOI: 10.1021/acssynbio.9b00149.

Table S1: Strains and plasmids used in this study; Table S2: Oligonucleotides used in this study; Table S3: Overview of all $xal_{Tc}$-variants isolated in the FACS campaign, which were characterized in detail; Figure S1: Performance of the *E. coli* pSenCA pBAD-$xal_{Tc}$ system; Figure S2: Influence of the inoculum size ($iOD_{600}$) on producer isolation efficiency; Figure S3: SDS-PAGE analysis of a typical $Xal_{Tc}$ purification (PDF)

## AUTHOR INFORMATION


### Corresponding Author

*Tel: +49 2461 61 2843. Fax: +49 2461 61 2710. E-mail: j.marienhagen@fz-juelich.de.

### ORCID

Jan Marienhagen: 0000-0001-5513-3730


### Author Contributions

L.K.F. designed the experiments, L.K.F. and S.S. conducted the experiments. L.K.F. and J.M. wrote the manuscript.

### Notes

The authors declare no competing financial interest.

## ACKNOWLEDGMENTS

The authors thank Alex Toftgaard Nielsen and Christian Bille Jendresen for providing PCBJ296. This project has received funding from the European Research Council (ERC) under the European Union's Horizon 2020 research and innovation programme (grant agreement No 638718).

## REFERENCES


(1) Daugherty, P. S., Iverson, B. L., and Georgiou, G. (2000) Flow cytometric screening of cell-based libraries. *J. Immunol. Methods 243*, 211−27.

(2) Zhang, J., Jensen, M. K., and Keasling, J. D. (2015) Development of biosensors and their application in metabolic engineering. *Curr. Opin. Chem. Biol. 28*, 1−8.

(3) Schallmey, M., Frunzke, J., Eggeling, L., and Marienhagen, J. (2014) Looking for the pick of the bunch: high-throughput screening of producing microorganisms with biosensors. *Curr. Opin. Biotechnol. 26*, 148−54.

(4) Snoek, T., Romero-Suarez, D., Zhang, J., Ambri, F., Skjoedt, M. L., Sudarsan, S., Jensen, M. K., and Keasling, J. D. (2018) An Orthogonal and pH-Tunable Sensor-Selector for Muconic Acid Biosynthesis in Yeast. *ACS Synth. Biol. 7*, 995−1003.

(5) Dietrich, J. A., Shis, D. L., Alikhani, A., and Keasling, J. D. (2013) Transcription factor-based screens and synthetic selections for microbial small-molecule biosynthesis. *ACS Synth. Biol. 2*, 47−58.

(6) Xu, P., Li, L., Zhang, F., Stephanopoulos, G., and Koffas, M. (2014) Improving fatty acids production by engineering dynamic pathway regulation and metabolic control. *Proc. Natl. Acad. Sci. U. S. A. 111*, 11299−304.

(7) Zhang, J., Sonnenschein, N., Pihl, T. P. B., Pedersen, K. R., Jensen, M. K., and Keasling, J. D. (2016) Engineering an NADPH/NADP+ Redox Biosensor in Yeast. *ACS Synth. Biol. 5*, 1546−1556.

(8) Chou, H. H., and Keasling, J. D. (2013) Programming adaptive control to evolve increased metabolite production. *Nat. Commun. 4*, 2595.

(9) Siedler, S., Schendzielorz, G., Binder, S., Eggeling, L., Bringer, S., and Bott, M. (2014) SoxR as a single-cell biosensor for NADPH-consuming enzymes in Escherichia coli. *ACS Synth. Biol. 3*, 41−7.

(10) Schendzielorz, G., Dippong, M., Grünberger, A., Kohlheyer, D., Yoshida, A., Binder, S., Nishiyama, C., Nishiyama, M., Bott, M., and Eggeling, L. (2014) Taking control over control: use of product sensing in single cells to remove flux control at key enzymes in biosynthesis pathways. *ACS Synth. Biol. 3*, 21−9.

(11) Binder, S., Schendzielorz, G., Stäbler, N., Krumbach, K., Hoffmann, K., Bott, M., and Eggeling, L. (2012) A high-throughput approach to identify genomic variants of bacterial metabolite producers at the single-cell level. *Genome Biol. 13*, R40.

(12) Mahr, R., Gätgens, C., Gätgens, J., Polen, T., Kalinowski, J., and Frunzke, J. (2015) Biosensor-driven adaptive laboratory evolution of l-valine production in Corynebacterium glutamicum. *Metab. Eng. 32*, 184−94.

(13) Xiao, Y., Bowen, C. H., Liu, D., and Zhang, F. (2016) Exploiting nongenetic cell-to-cell variation for enhanced biosynthesis. *Nat. Chem. Biol. 12*, 339−44.

(14) Dietrich, J. A., McKee, A. E., and Keasling, J. D. (2010) High-throughput metabolic engineering: advances in small-molecule screening and selection. *Annu. Rev. Biochem. 79*, 563−90.

(15) Bertani, G. (1951) Studies on lysogenesis. I. The mode of phage liberation by lysogenic Escherichia coli. *J. Bacteriol. 62*, 293−300.




DOI: 10.1021/acssynbio.9b00149
*ACS Synth. Biol.* 2019, 8, 1847−1857

(16) Durfee, T., Nelson, R., Baldwin, S., Plunkett, G., Burland, V., Mau, B., Petrosino, J. F., Qin, X., Muzny, D. M., Ayele, M., Gibbs, R. A., Csörgo, B., Pósfai, G., Weinstock, G. M., and Blattner, F. R. (2008) The complete genome sequence of Escherichia coli DH10B: insights into the biology of a laboratory workhorse. *J. Bacteriol. 190*, 2597−606.
(17) Kensy, F., Zang, E., Faulhammer, C., Tan, R.-K., and Büchs, J. (2009) Validation of a high-throughput fermentation system based on online monitoring of biomass and fluorescence in continuously shaken microtiter plates. *Microb. Cell Fact. 8*, 31.
(18) Funke, M., Diederichs, S., Kensy, F., Müller, C., and Büchs, J. (2009) The baffled microtiter plate: increased oxygen transfer and improved online monitoring in small scale fermentations. *Biotechnol. Bioeng. 103*, 1118−28.
(19) Sambrook, J., and Russel, D. W. (2001) *Molecular Cloning A Lab Manual 3*, Cold Spring Harbor Laboratory Press, New York.
(20) Gibson, D. G., Young, L., Chuang, R.-Y., Venter, J. C., Hutchison, C. A., and Smith, H. O. (2009) Enzymatic assembly of DNA molecules up to several hundred kilobases. *Nat. Methods 6*, 343−345.
(21) Dower, W. J., Miller, J. F., and Ragsdale, C. W. (1988) High efficiency transformation of E. coli by high voltage electroporation. *Nucleic Acids Res. 16*, 6127−45.
(22) Yu, D., Ellis, H. M., Lee, E. C., Jenkins, N. A., Copeland, N. G., and Court, D. L. (2000) An efficient recombination system for chromosome engineering in Escherichia coli. *Proc. Natl. Acad. Sci. U. S. A. 97*, 5978−83.
(23) Datsenko, K. A., and Wanner, B. L. (2000) One-step inactivation of chromosomal genes in Escherichia coli K-12 using PCR products. *Proc. Natl. Acad. Sci. U. S. A. 97*, 6640−5.
(24) Jensen, S. I., Lennen, R. M., Herrgård, M. J., and Nielsen, A. T. (2016) Seven gene deletions in seven days: Fast generation of Escherichia coli strains tolerant to acetate and osmotic stress. *Sci. Rep. 5*, 17874.
(25) Jensen, S. I., and Nielsen, A. T. (2018) Multiplex Genome Edititing in *Escherichia coli*, in *Synthetic Metabolic Pathways* (Jensen, M. K., and Keasling, J. D., Eds.), pp 119−129, Springer Science + Business Media.
(26) Freiherr von Boeselager, R., Pfeifer, E., and Frunzke, J. (2018) Cytometry meets next-generation sequencing - RNA-Seq of sorted subpopulations reveals regional replication and iron-triggered prophage induction in Corynebacterium glutamicum. *Sci. Rep. 8*, 14856.
(27) Watts, K. T., Mijts, B. N., Lee, P. C., Manning, A. J., and Schmidt-Dannert, C. (2006) Discovery of a substrate selectivity switch in tyrosine ammonia-lyase, a member of the aromatic amino acid lyase family. *Chem. Biol. 13*, 1317−26.
(28) Milke, L., Aschenbrenner, J., Marienhagen, J., and Kallscheuer, N. (2018) Production of plant-derived polyphenols in micro-organisms: current state and perspectives. *Appl. Microbiol. Biotechnol. 102*, 1575−1585.
(29) Kallscheuer, N., Menezes, R., Foito, A., da Silva, M. H., Braga, A., Dekker, W., Sevillano, D. M., Rosado-Ramos, R., Jardim, C., Oliveira, J., Ferreira, P., Rocha, I., Silva, A. R., Sousa, M., Allwood, J. W., Bott, M., Faria, N., Stewart, D., Ottens, M., Naesby, M., Nunes Dos Santos, C., and Marienhagen, J. (2019) Identification and Microbial Production of the Raspberry Phenol Salidroside that Is Active against Huntington's Disease. *Plant Physiol. 179*, 969−985.
(30) Koopman, F., Beekwilder, J., Crimi, B., van Houwelingen, A., Hall, R. D., Bosch, D., van Maris, A. J., Pronk, J. T., and Daran, J.-M. (2012) De novo production of the flavonoid naringenin in engineered Saccharomyces cerevisiae. *Microb. Cell Fact. 11*, 155.
(31) Santos, C. N. S., Koffas, M., and Stephanopoulos, G. (2011) Optimization of a heterologous pathway for the production of flavonoids from glucose. *Metab. Eng. 13*, 392−400.
(32) Zhou, S., Liu, P., Chen, J., Du, G., Li, H., and Zhou, J. (2016) Characterization of mutants of a tyrosine ammonia-lyase from Rhodotorula glutinis. *Appl. Microbiol. Biotechnol. 100*, 10443−10452.
(33) Eudes, A., Juminaga, D., Baidoo, E. E. K., Collins, F., Keasling, J. D., and Loqué, D. (2013) Production of hydroxycinnamoyl anthranilates from glucose in Escherichia coli. *Microb. Cell Fact. 12*, 62.
(34) Lin, Y., and Yan, Y. (2012) Biosynthesis of caffeic acid in Escherichia coli using its endogenous hydroxylase complex. *Microb. Cell Fact. 11*, 42.
(35) Kallscheuer, N., Vogt, M., Stenzel, A., Gätgens, J., Bott, M., and Marienhagen, J. (2016) Construction of a Corynebacterium glutamicum platform strain for the production of stilbenes and (2S)-flavanones. *Metab. Eng. 38*, 47−55.
(36) Díaz, E., Ferrández, A., Prieto, M. A., and García, J. L. (2001) Biodegradation of aromatic compounds by Escherichia coli. *Microbiol. Mol. Biol. Rev. 65*, 523−69.
(37) Díaz, E., Ferrández, A., and García, J. L. (1998) Characterization of the hca cluster encoding the dioxygenolytic pathway for initial catabolism of 3-phenylpropionic acid in Escherichia coli K-12. *J. Bacteriol. 180*, 2915−2923.
(38) Kovářová, K., Käch, A., Chaloupka, V., and Egli, T. (1996) Cultivation of Escherichia coli with mixtures of 3-phenylpropionic acid and glucose: Dynamics of growth and substrate consumption. *Biodegradation 7*, 445−453.
(39) Turlin, E., Perrotte-Piquemal, M., Danchin, A., and Biville, F. (2001) Regulation of the early steps of 3-phenylpropionate catabolism in Escherichia coli. *J. Mol. Microbiol. Biotechnol. 3*, 127−133.
(40) Jendresen, C. B., Stahlhut, S. G., Li, M., Gaspar, P., Siedler, S., Förster, J., Maury, J., Borodina, I., and Nielsen, A. T. (2015) Novel highly active and specific tyrosine ammonia-lyases from diverse origins enable enhanced production of aromatic compounds in bacteria and yeast. *Appl. Environ. Microbiol. 81*, 4458.
(41) Guzman, L. M., Belin, D., Carson, M. J., and Beckwith, J. (1995) Tight regulation, modulation, and high-level expression by vectors containing the arabinose PBAD promoter. *J. Bacteriol. 177*, 4121−30.
(42) Desai, T. A., and Rao, C. V. (2010) Regulation of arabinose and xylose metabolism in Escherichia coli. *Appl. Environ. Microbiol. 76*, 1524−32.
(43) Crane, R. K. (1977) The gradient hypothesis and other models of carrier-mediated active transport, in *Reviews of Physiology, Biochemistry and Pharmacology*, Vol. *78*, pp 99−159, Springer-Verlag, Berlin/Heidelberg.
(44) Eggeling, L., Bott, M., and Marienhagen, J. (2015) Novel screening methods—biosensors. *Curr. Opin. Biotechnol. 35*, 30−36.
(45) Mustafi, N., Grünberger, A., Kohlheyer, D., Bott, M., and Frunzke, J. (2012) The development and application of a single-cell biosensor for the detection of l-methionine and branched-chain amino acids. *Metab. Eng. 14*, 449−57.
(46) Lange, C., Mustafi, N., Frunzke, J., Kennerknecht, N., Wessel, M., Bott, M., and Wendisch, V. F. (2012) Lrp of Corynebacterium glutamicum controls expression of the brnFE operon encoding the export system for L-methionine and branched-chain amino acids. *J. Biotechnol. 158*, 231−41.
(47) Mannan, A. A., Liu, D., Zhang, F., and Oyarzún, D. A. (2017) Fundamental Design Principles for Transcription-Factor-Based Metabolite Biosensors. *ACS Synth. Biol. 6*, 1851−1859.
(48) Rebets, Y., Schmelz, S., Gromyko, O., Tistechok, S., Petzke, L., Scrima, A., and Luzhetskyy, A. (2018) Design, development and application of whole-cell based antibiotic-specific biosensor. *Metab. Eng. 47*, 263−270.
(49) Jha, R. K., Kern, T. L., Fox, D. T., and Strauss, C. E. M. (2014) Engineering an Acinetobacter regulon for biosensing and high-throughput enzyme screening in E. coli via flow cytometry. *Nucleic Acids Res. 42*, 8150−8160.
(50) Siedler, S., Khatri, N. K., Zsohár, A., Kjærbølling, I., Vogt, M., Hammar, P., Nielsen, C. F., Marienhagen, J., Sommer, M. O. A., and Joensson, H. N. (2017) Development of a Bacterial Biosensor for Rapid Screening of Yeast p-Coumaric Acid Production. *ACS Synth. Biol. 6*, 1860−1869.


DOI: 10.1021/acssynbio.9b00149
*ACS Synth. Biol.* 2019, 8, 1847−1857

(51) Baret, J.-C., Miller, O. J., Taly, V., Ryckelynck, M., El-Harrak, A., Frenz, L., Rick, C., Samuels, M. L., Hutchison, J. B., Agresti, J. J., Link, D. R., Weitz, D. A., and Griffiths, A. D. (2009) Fluorescence-activated droplet sorting (FADS): efficient microfluidic cell sorting based on enzymatic activity. *Lab Chip 9*, 1850−8.

(52) Wagner, J. M., Liu, L., Yuan, S.-F., Venkataraman, M. V., Abate, A. R., and Alper, H. S. (2018) A comparative analysis of single cell and droplet-based FACS for improving production phenotypes: Riboflavin overproduction in Yarrowia lipolytica. *Metab. Eng. 47*, 346−356.

(53) Siegele, D. a, and Hu, J. C. (1997) Gene expression from plasmids containing the araBAD promoter at subsaturating inducer concentrations represents mixed populations. *Proc. Natl. Acad. Sci. U. S. A. 94*, 8168−72.

(54) Khlebnikov, A., Skaug, T., and Keasling, J. D. (2002) Modulation of gene expression from the arabinose-inducible araBAD promoter. *J. Ind. Microbiol. Biotechnol. 29*, 34−7.



DOI: 10.1021/acssynbio.9b00149
*ACS Synth. Biol.* 2019, 8, 1847−1857